Polymer-Assisted Direct Deposition of Uniform Carbon Nanotube Bundle Networks for High Performance Transparent Electrodes

Sondra L. Hellstrom,[†] Hang Woo Lee,[‡] and Zhenan Bao[‡,*]

[†]Department of Applied Physics, Stanford University, Stanford, California 94305, and [‡]Department of Chemical Engineering, Stanford University, Stanford, California 94305

ABSTRACT Flexible transparent electrodes are crucial for touch screen, flat panel display, and solar cell technologies. While carbon nanotube network electrodes show promise, characteristically poor dispersion properties have limited their practicality. We report that addition of small amounts of conjugated polymer to nanotube dispersions enables straightforward fabrication of uniform network electrodes by spin-coating and simultaneous tuning of parameters such as bundle size and density. After treatment in thionyl chloride, electrodes have sheet resistances competitive with other reported carbon nanotube based transparent electrodes to date.

KEYWORDS: transparent conductors · nanotubes · composites · solution processed · solar cells

Transparent conducting materials are critical for use in touch screens, solar cells, and flat panel displays.[1] The most common material at present for fabricating such electrodes is indium tin oxide (ITO), but for low-cost or flexible electronics, such as those using organic semiconductors, ITO has well-known disadvantages including high-temperature processing steps that are incompatible with plastic substrates,[2] brittleness,[3] and rapidly increasing costs of scarce materials.[4] An ideal replacement should be inexpensive, flexible, thin, and uniform over all size scales, with a sheet resistance of 50 Ω/sq or less at 85% transparency.[5] It should also ideally be amenable to deposition directly and uniformly from solution onto the surface of interest in a scalable fashion, for example *via* inkjet printing, airbrushing, dip-coating, or spin-coating.

No currently known transparent conducting material completely satisfies this set of specifications. Metal grating[6] and nanowire mesh[7] electrodes satisfy the sheet resistance and flexibility requirements, but both have nonuniform surface coverage on the nanometer scale; the former requires lithography for fabrication, while the latter suffers from high roughness, as the nanowires can stack hundreds of nanometers high. Additionally, surface environmental stability is a concern with some metals and for use with an organic active layer. Conducting polymer electrodes can have a reduced or absent surface dipole barrier to charge injection compared with inorganic electrodes.[8] However, electrodes based on these conducting polymers, such as polyaniline[9] or PEDOT,[10] do not transmit much visible light when layered thickly enough to be sufficiently conducting. Reduced graphene oxide electrodes, while less studied, require high-temperature annealing and are currently about an order of magnitude too resistive.[11]

One of the more promising candidates for transparent electrodes is the carbon nanotube (CNT) network. While the detailed charge transport properties of such electrodes are not well-understood, there are at least two problems that require addressing. The first difficulty is large intertube junction resistances, especially between metallic and semiconducting tubes.[12] This can be potentially mitigated by using chirally sorted nanotubes,[13−15] by introducing alignment into tube networks,[16−18] or by treating unsorted tubes following network formation, typically with HNO_3 and/or $SOCl_2$.[19−21] The second is that direct deposition of CNT networks from solution has proven challenging due to poor dispersion, leading to inhomogeneous, inefficiently networked films. Fabricating the films on a vacuum filter and transferring them to the required substrate with the assistance of surfactants[22−25] and/or conjugated polymer[26] is the most reliable technique at

*Address correspondence to shells@stanford.edu, zbao@stanford.edu.

Received for review March 11, 2009 and accepted April 29, 2009.

Published online May 7, 2009.
10.1021/nn9002456 CCC: $40.75

present, giving best performances of 120 Ω/sq at 80% transparency undoped,[23] 160 Ω/sq at 87% doped,[25] or 80 Ω/sq at 75% in polymer composites;[26] however, this method typically requires use of large amounts of surfactant that needs to be removed, and it makes films limited to the size of the membrane filter and involves a transfer printing step.

By comparison, spray-coating[5,27] and rod-coating[28] a carbon nanotube/surfactant solution are direct deposition approaches to nanotube network formation, but the former is highly susceptible to inhomogeneity and both require centrifugation or use of a large weight percent of surfactant to achieve good dispersion. After acid treatment, shown to remove much of the surfactant, film performance in the case of spray-coating is similar to the vacuum-filtered samples. Recently, a report of spin-coated CNT transparent conducting electrodes, deposited without surfactant, achieved the requisite dispersion by sonicating tubes in dichloroethane for 12 h followed by centrifugation; even then, the dispersion was unreliable.[29] Despite containing no surfactant, their films exhibited a similar reduction in sheet resistance upon treatment with nitric acid, and they obtained similar end results of about 85 Ω/sq at 80% transparency doped (222 Ω/sq undoped).

It is known that CNTs are more easily dispersed in chlorinated solvents in the presence of poly-3-alkylthiophenes (P3AT) such as regioregular poly-3-hexylthiophene (rr-P3HT) or poly-3-dodecylthiophene (P3DT).[30,31] While much study has been made of rr-P3HT:CNT composites, the focus is usually on the effect of a smaller weight percent of nanotubes added to a majority rr-P3HT active layer.[32−35] Due to the more conducting nature of these polymers compared with typical surfactants like SDS, and due to their ability to disperse carbon nanotubes at lower relative concentrations, it may be anticipated that such films have great promise as uniform transparent electrodes. However, no work known to the authors to date has actually investigated the properties of composite films of greater than 50 wt % carbon nanotubes.

RESULTS AND DISCUSSION

Nanotube Composite Network Electrode Fabrication: We demonstrate here a simple, reliable method for forming uniform carbon nanotube network electrodes deposited directly onto the surface of interest *via* spin-coating or drop-casting. When spin-cast onto substrates, well-dispersed nanotubes in low concentrations are difficult to build up to sufficient density for electrode applications, while higher concentrations form nonuniform clumps of bundles. By introducing conjugated polymers such as rr-P3HT or rr-P3DT to carbon nanotube suspensions in chloroform, we significantly improve both the dispersion in solution and the quality of spin-coated CNT films on glass and polyethylene terephthalate (PET).

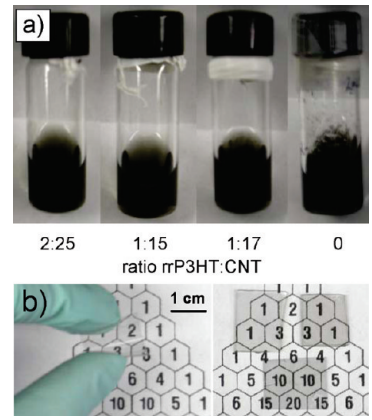

Figure 1. Photographs of (a) rr-P3HT:CNT composite solutions with various weight ratios in chloroform following sonication and (b) composite films of different thicknesses following spin-coating. The left image shows a network of 89% transmittance at 550 nm on PET. The right image shows the same film flat (bottom) as well as two networks on glass, of 92 and 87% transmittance at 550 nm.

We use arc-discharge nanotubes in this study, as they are known to have superior conductivity in networks compared with tubes synthesized by other methods.[25] These nanotubes are purified to remove amorphous carbon and other contaminants according to literature procedures.[36] After purification, sonication power and time are limited in this work to 60 min or less and 180 W or less to minimize tube damage and cutting. Above an initial weight ratio of about 1:15 rr-P3HT:CNT in chloroform, it is straightforward within these sonication limits to disperse 80−100 μg CNT/mL so that it will appear uniform by eye. Much below this ratio, aggregates of nanotubes in the solvent will still be observable (Figure 1b). The stabilities of these dispersions have not been comprehensively investigated but are sufficient for spin-coating shortly after sonication. No appreciable difference in behavior is observed using rr-P3DT, except that the minimal ratio required for dispersion increases to about 2:25.

Controlling polymer concentration and solvent enables variation of tube bundle size and film roughness as qualitatively observable by atomic force microscopy, adding an additional degree of freedom to tune film morphology toward specific applications. Such tuning may be done independently of bundle density since the latter is controllable separately by changing the volume of dispersion deposited during spin-coating, allowing a variety of film thicknesses (Figure 1a). Spin-coating is straightforward, but film thickness is often difficult to quantify in many cases due to sparse bundle coverage, so optical density of the film at 550 nm is typically used as a substitute metric. After deposition and annealing as described in the Methods section, all samples are washed in chloroform for 10 min to remove as much excess polymer as possible.

Nanotube Composite Network Morphology: The morphologies of rr-P3HT:CNT films vary considerably as a func-

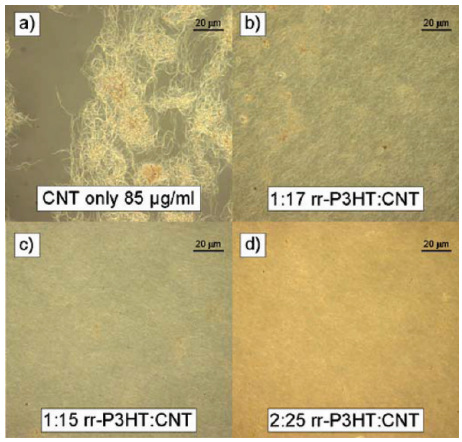

Figure 2. (a) Optical micrograph of a nanotube network on glass, of approximately 76% transmittance at 550 nm, spin-cast from an 85 μg/mL CNT solution in chloroform containing no polymer. (b−d) Identical micrographs, spin-cast from rr-P3HT:CNT composite solutions in chloroform containing the indicated relative weight ratios. Transmittances at 550 nm are 79, 80, and 83%, respectively.

tion of relative weight ratio. A control solution containing no polymer and 80−100 μg CNT/mL, spin-coated onto glass, has as mentioned earlier a very uneven morphology, with dense aggregates of large tube bundles (up to 70 nm in diameter) in some places and sparse regions in between. This is clearly visible under 50× microscope objective (Figure 2a) and is consistent with atomic force microscopy images of the same films (Figure 3a).

In contrast, as observed by atomic force and optical microscopy, the composite films cover the substrate surface uniformly with a distribution of both bundles and single tubes. As the rr-P3HT concentration increases from none to 1:15 to 1:5, the proportion of single tubes and small bundles (diameter less than about 5 nm) relative to all the observable bundles in the image also increases (Figure 3b,c), and the presence of visible bundle aggregates both in solution and on substrate diminishes (Figures 1a and 2b−d). While not shown, similar behavior is found to be true on flexible plastic substrates. Although the largest bundle sizes in the composites, about 20−25 nm diameter, are smaller than in the control, they are still larger than those in many reported high-performance nanotube network electrodes.[23,29,37]

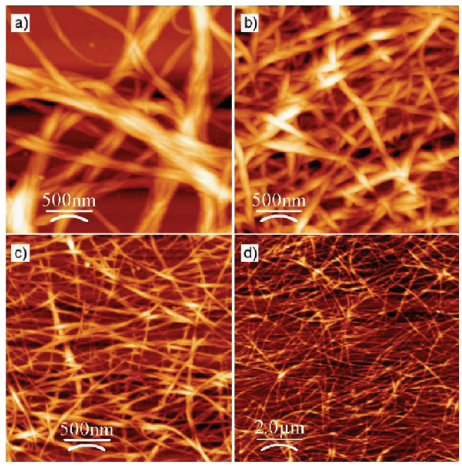

Figure 3. Atomic force microscopy images (2.5 μm) of nanotube networks on glass, spin-cast from (a) 0:1, (b) 1:15, and (c) 1:5 rr-P3HT:CNT composite solutions in chloroform. The rms roughness values and the % transmittances at 550 nm are 28 nm and ~75%; 17 nm and 80%; 12 nm and 88%, respectively. (d) A 1:15 ratio composite film on a larger scale (10 μm) for comparison, with a rms roughness of 12 nm and a % transmittance of 91% at 550 nm.

Previous reports of spin-coated carbon nanotube networks have reported that the spin-coating process results in an imperfect but marked radial alignment of the carbon nanotubes on the substrate surface.[36] We find that this is also often true in the spin-coating of the composite bundles, but only at bundle densities sufficiently low that the tubes are touching the surface directly. As the film thickness increases, the consistency of observed alignment decreases. Nevertheless, this alignment might be anticipated to improve the performance of spin-coated films relative to those made with other techniques, particularly for more highly transparent electrodes.

Optical and Raman Spectroscopy of Nanotube Composite Networks: Studying the transmittance spectra of washed rr-P3HT:CNT composite films reveals that the dominant absorption for all composite ratios is from the nanotubes and, in particular, from the tail of the π-plasmon resonance (Figure 4a);[38] however, small increases in absorbance reveal the presence of the conjugated polymer in the 350−650 nm range, along with broad nanotube M1 and S2 transitions. For initial polymer weight ratios of 1:5 or smaller, the decrease in transmittance due to the explicit presence of the polymer is 2% or less; the presence of the polymer in the 1:1 case has a more substantial impact (Figure 4b).

Treating the nanotube films by immersion in $SOCl_2$ for 12 h causes substantial changes in nanotube absorption spectra, particularly *via* the bleaching of the CNT optical transitions due to doping. This is already well-documented.[39,40] However, in this work, there is additionally the complicating factor of the presence of the conjugated polymer. We find that P3HT absorption diminishes with $SOCl_2$ treatment, indicating that the polymer remaining in the composite films is further removed or damaged by the $SOCl_2$ (Figure 4c).

To confirm both the scaling of residual presence of rr-P3HT in the composites as a function of polymer:CNT ratio, and to better understand the role of the thionyl chloride treatment on the composite network, we use Raman spectroscopy to characterize composite networks of varying P3HT content. Raman spectra of both carbon nanotubes[41] and P3HT[42] are well-characterized. In the control with no polymer, the radial breathing mode (172 nm), D-band (1328 nm), and G-band (1592 nm) are clearly evident. In the untreated composite films (Figure 5a,b), the more intense P3HT Raman peaks

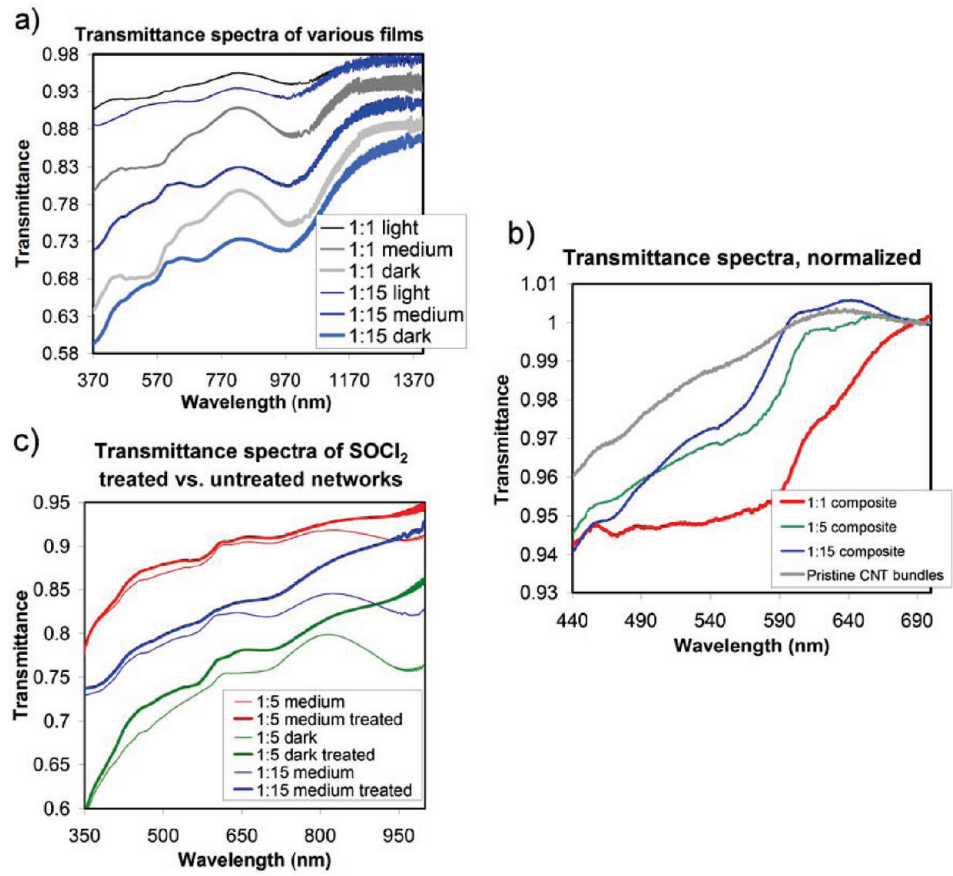

Figure 4. (a) UV−vis spectra of 1:15 and 1:1 rr-P3HT:CNT composite films of three different thicknesses (light, medium, dark). (b) Detail of spectra of 0:1, 1:15, 1:5, and 1:1 rr-P3HT:CNT composite films, normalized to the ~690 nm M1 nanotube peak to highlight differences in polymer absorption. The slope of the 1:15 composite line is steepest because it is the darkest actual film. (c) UV−vis spectra of composite films of two different thicknesses (medium, dark) following $SOCl_2$ treatment.

(723, 1000, 1090, 1207, 1378, and 1440 nm, in particular) become detectable at a 1:5 rr-P3HT:CNT ratio; more detailed spectral structure is clearly visible in a 1:1 composite. Most peak positions are invariant as the P3HT concentration changes; however, in particular, the $C_\beta-C_{\beta'}$ ring stretching P3HT mode at approximately 1378 cm^{-1} shifts over 10 cm^{-1} between the 1:15 and 1:1 composites.

After treating the composites with $SOCl_2$, the Breit−Wigner−Fano resonance characteristic of metallic tubes around the low-frequency portion of the G-band is suppressed, and the G-band itself is blue-shifted (Figure 5c,d). This is consistent with previous findings for $SOCl_2$-treated pristine tubes.[21] However, we also find that the rr-P3HT peaks are suppressed, an effect which is particularly visible at the most intense P3HT peaks at 1378 and 1440 cm^{-1}. This cannot be due to a removal of material from the film overall, as the nanotube D- and G-band intensities do not commensurately decrease. The relative decrease in intensity of these P3HT ring-stretching modes indicates that one additional effect of the $SOCl_2$ is a denaturing or further removal of P3HT from the composite, and this itself may contribute to improvement in electrical performance of the films irrespective of nanotube doping.

Nanotube Composite Network Electrical Measurements: Ultimately, the utility of a nanotube network electrode is judged by its conductance for a particular transparency. These data are shown in Figure 6 for various ratio composites, both untreated and post-treated, and compared with current best reported values for nanotube network electrodes found by the authors in the literature.

The untreated 1:5 films had moderately poorer performance, and the 1:1 films had significantly poorer performance, compared with the 1:15 ratio composites. Samples with greater than 50% weight carbon nanotubes consistently outperformed nanotube-only controls. The $SOCl_2$ treatment had a greater impact on the films with higher polymer content, improving sheet resistance by an average factor of about 4 compared with 2.6, such that the treated 1:5 and 1:15 ratio composite films ultimately had similar performance when tested shortly after treatment.

After $SOCl_2$ treatment, the networks are competitive with those produced using other more involved methods involving vacuum filtration (which achieve at best 160 Ω/sq at 87% transmittance)[25] or lengthy sonication and centrifugation (at best 85 Ω/sq at 80% transmittance).[29] A 1:15 ratio rr-P3HT:CNT composite has a

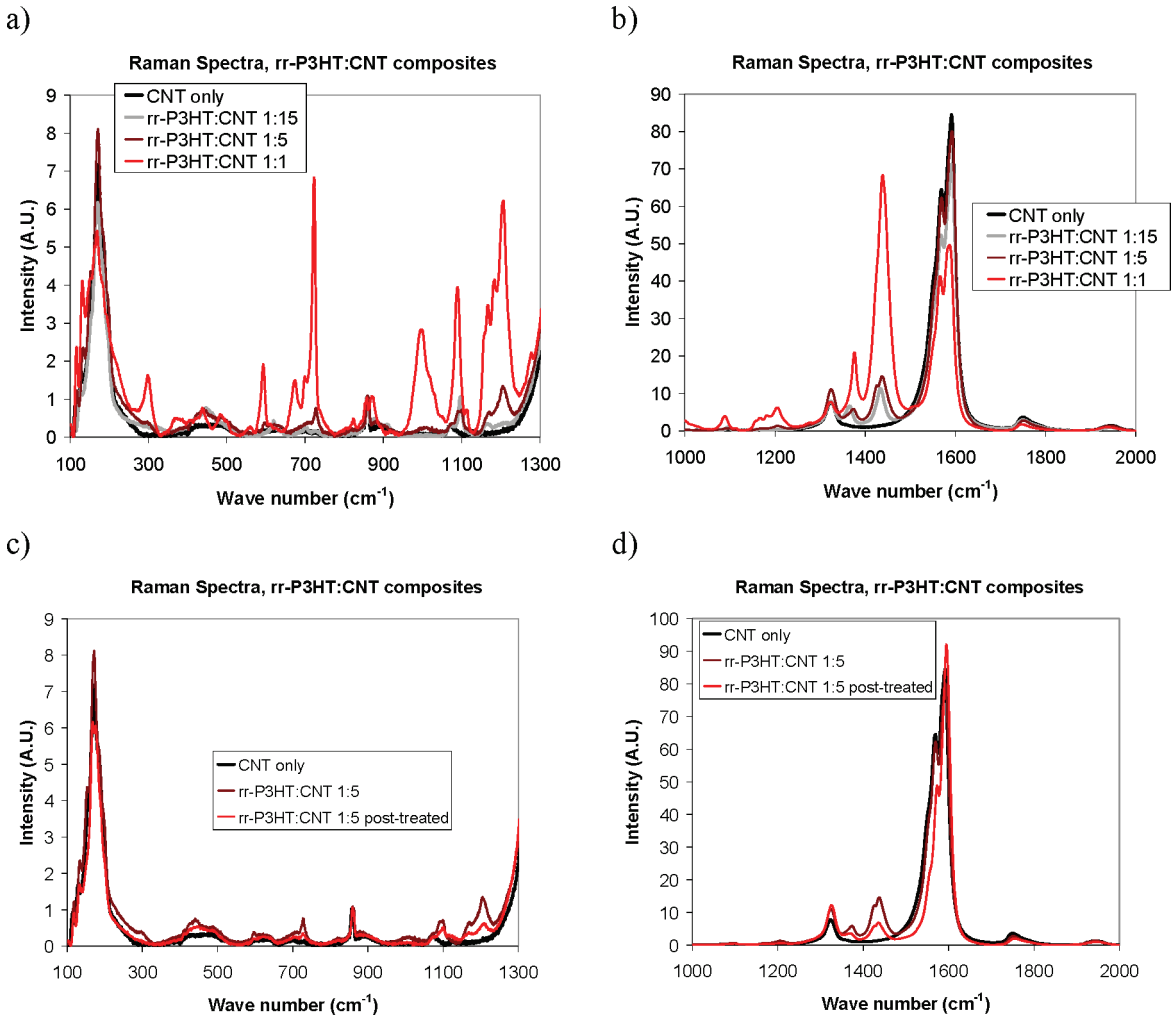

Figure 5. Raman spectra of various rr-P3HT:CNT composite films as a function of relative weight ratio, (a) 100−1300 cm^{-1} and (b) 1000−2000 cm^{-1}, and similar Raman spectra of rr-P3HT:CNT 1:5 composite films, before and after $SOCl_2$ treatment, (c) 100−1300 cm^{-1} and (d) 1000−2000 cm^{-1}, compared with a CNT-only control. Intensities of all spectra are normalized to the graphite out-of-plane transverse optical phonon peak, constant at 860 cm^{-1} for arc-discharge tubes irrespective of excitation energy or tube chirality. This was selected because of its constancy and because many of the composite films are thick enough to prevent observation of any substrate peaks.

sheet resistance of 170 Ω/sq at 81% transmittance, and a 1:5 ratio rr-P3DT:CNT composite has a sheet resistance of about 80 Ω/sq at 72% transmittance. It should be noted, however, that the measured sheet resistance for a nanotube network varies sensitively depending on the history of the sample and its constituent material and also on the details of how the measurement is made—the type, position, and geometry of the electrodes.[39,43] This makes comparison with literature values difficult, especially when measurement details therein are not reported.

If the thickness of a metallic film is small compared with the wavelength of light, the relationship between its transmittance and sheet resistance in air may be modeled by

$$T(\lambda) = \left(1 + \frac{188.5}{R_S}\frac{\sigma_{op}(\lambda)}{\sigma_{dc}}\right)^{-2}$$

where λ is the wavelength of light at which the properties are measured (typically 550 nm) and σ_{op} and σ_{dc} are the optical and DC conductivities of the material.[26,44] In the framework of this model, σ_{op}/σ_{dc} may be used as a figure of merit for the performance of a nanotube network. On the basis of measured transmittance and sheet resistance, the best treated composite films have $\sigma_{op}/\sigma_{dc} \sim 13$. Calculations of σ_{op}/σ_{dc} for various films in Figure 6 may be found in the Supporting Information.

Excess polymer may hinder the network electrodes in several ways. First, it is strongly absorbing at 550 nm, without conducting commensurately with the carbon nanotubes. Second, beyond acting as simply an absorbing agent, the polymer may actively interfere with conduction between nanotubes, adding a series resistance component. The role of the $SOCl_2$ in this context is likely both to dope the nanotubes and to dope, destroy, or remove excess polymer. While the relative importance of these contributions is yet to be determined, the varied responses of films of varied polymer con-

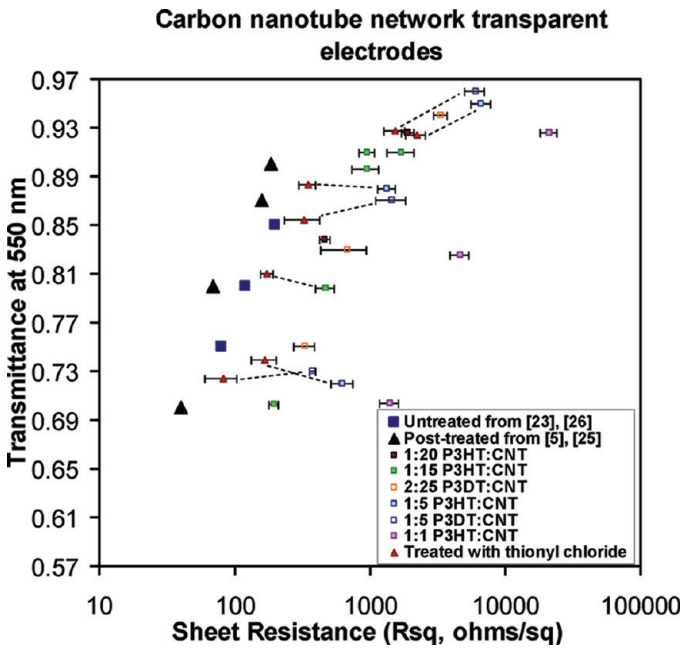

Figure 6. Sheet resistance (R_{sq}) *versus* transmittance at 550 nm for spin-coated composite electrodes with various weight ratios of P3AT, compared with the best reported literature nanotube networks, both untreated,[23] untreated in composites,[26] and treated with HNO_3[5] or $SOCl_2$.[25] Error bars indicate standard error computed from repeated measurements at different locations on a single substrate. The dashed lines connect measurements on identical substrates, before and after $SOCl_2$ treatment.

tent to the $SOCl_2$ treatment support the presence or even prominence of the latter effect.

The polymer may further impact the performance of the nanotube networks through its influence on network morphology. While improved overall uniformity clearly improves device performance, effects of the observed changes in bundle size on performance are less clear. Certainly, while it has been thought that smaller nanotube bundles or single tubes are preferable,[23,29,37] this work clearly demonstrates that competitive electrodes to date can be fabricated despite the presence of bundles of 40 nm in diameter or more.

CONCLUSIONS

In conclusion, adding P3AT to carbon nanotube dispersions in quantities minimally sufficient to disperse the nanotubes enabled straightforward fabrication of uniform CNT network transparent conducting electrodes *via* spin-coating onto glass. After subsequent treatment of these networks in $SOCl_2$, sheet resistances of about 80 Ω/sq at 72% transmittance at 550 nm were obtained. Preliminary results indicate that this method is extensible to using other soluble conjugated polymers such as poly[2-methoxy-5-(2′-ethylhexyloxy)-1,4-phenylene vinylene] (MEH-PPV). Other substrates including PET may also be used. Without optimization, using 1:15 ratio P3HT composites spin-coated onto plastic substrates and the same procedures described earlier, films performed similar to but slightly (a factor of ~1.2) worse than those deposited on glass under similar conditions. The technique ultimately provides an easy, reliable, scalable, plastics-compatible method for fabricating flexible transparent electrodes directly from solution onto the substrate of interest.

METHODS

Nanotube Purification: Arc-discharge carbon nanotubes are purchased from ILJIN Nanotech, grade ASP-100F; 80 mg of these tubes is mixed with 2 g of J.T. Baker sodium dodecyl sulfate (SDS) and 200 mL of Invitrogen 0.1 μm filtered ultrapure water. This mixture is placed in an ice water bath and sonicated in a Cole-Parmer ultrasonic cup-horn sonicator for 30 min at 750 W. After sonication, the dispersion is centrifuged at 15 000 rpm for 4 h at 4 °C in a Sorvall RC5C Plus centrifuge, and the supernatant decanted. The supernatant is diluted with anhydrous acetone, which dissociates the SDS from the nanotubes, and centrifuged to collect the precipitated tubes. This process of acetone rinsing followed by precipitate collection is repeated four times. Finally, the mixture is filtered through a Millipore 0.45 μm pore size PTFE membrane to collect the nanotubes. The tubes form a sheet on top of the filter, which is then peeled off and dried at 50 °C under vacuum overnight.

Composite Solution Preparation: One to 1.5 mg of the SWNTs prepared during nanotube purification is dispersed in chloroform at a concentration of 100 μg/mL, by sonicating at 180 W for 30 min in an ice bath, using the same Cole-Parmer ultrasonic cup-horn sonicator as during the purification step. Separately, a few mg of rr-P3HT from Sigma Aldrich is dissolved in 4 mL of chloroform under gentle heating and shaking. The relevant quantity of rr-P3HT is then added to 2 mL of the nanotube dispersion using a glass microliter syringe, and the mixture is again sonicated at 180 W for 30−60 min, until the suspension is uniform to the eye. The total volume of solution is then refreshed to 2 mL by adding additional chloroform.

Substrate Preparation and Spin-Coating: A 1.5 cm × 1.5 cm cut display-grade TFT glass (Eagle glass by Corning) is cleaned by placing in chloroform and then in a Branson 3510 100 W/42 kHz ultrasonic cleaner for 10 min, then switching the solvent to ethanol and repeating. This is followed by drying the substrates under a nitrogen stream and placing them in a Jelight Model 42 UV−Ozone cleaner for 20 min. A substrate is set spinning at 7000 rpm, and the predetermined amount of solution is dropped, one drop at a time, onto the substrate using a glass pipet. After spin-coating, the back of the substrate is cleaned with methanol, and the sample is annealed at about 120 °C on a hot plate, soaked in chloroform for an additional 10 min, and dried to remove any accessible excess polymer.

Thionyl Chloride Treatment: After initial electrical measurements, samples are placed individually in glass vials face-up and thionyl chloride (Alfa Aesar, 99+%) is carefully introduced to the vial *via* glass pipet until the sample is fully immersed. Samples are left loosely covered for 12 h and then removed and carefully dried under gentle nitrogen stream. Post-treatment electrical data are taken within 1 h of treatment to avoid concerns of instability of the doped films.[20]

Instrumentation: Optical microscopy was taken under a 50× objective with the substrate suspended to prevent the support from being visible through the glass. Atomic force microscopy was taken using a Veeco Multimode SPM in tapping mode. Transmittances and optical spectra were measured by a Cary 6000i UV−vis−NIR spectrophotometer (Varian, Inc.). Micro-Raman measurements (LabRam Aramis, Horiba Jobin Yvon) were obtained at 633 nm excitation at 100× magnification and 1 μm spot size, and at least four spectra were obtained per

sample. Gold electrodes of nominally 50 nm thickness as monitored by QCM were deposited *via* thermal evaporation (Angstrom Engineering, Inc.) through a cut transparency film shadow mask, at a rate of 0.3−0.6 Å/s. The electrodes were in the form of line arrays with a 2 mm × 2 mm central channel. Electrical measurements were taken using a Keithley 4200SCS semiconductor parameter analyzer and a standard probe station setup. After measuring, all sheet resistance values were multiplied by a factor of 2.5, which represents the average empirically determined effect of fringe electric field on this electrode geometry.

Acknowledgment. S.L.H. would like to thank the National Science Foundation Graduate Research Fellowship Program for funding. Additionally, Dr. Melburne LeMieux, Mike Rowell, Dr. Mark Topinka, and Dr. Mike McGehee provided useful insight. We would like to thank Stanford University Global Climate and Energy Project (GCEP) and Samsung Advanced Institute of Technology. This publication was partially based on work supported by the Center for Advanced Molecular Photovoltaics (Award No KUS-C1-015-21), made by King Abdullah University of Science and Technology (KAUST).

Supporting Information Available: Additional experimental details. This material is available free of charge *via* the Internet at http://pubs.acs.org.

REFERENCES AND NOTES

1. Gruner, G. Carbon Nanotube Films for Transparent and Plastic Electronics. *J. Mater. Chem.* **2006**, *16*, 3533–3539.
2. Gonçalves, G.; Elangovan, E.; Barquinha, P.; Pereira, L.; Martins, R.; Fortunato, E. Influence of Post-Annealing Temperature on the Properties Exhibited by ITO, IZO and GZO Thin Films. *Thin Solid Films* **2007**, *515*, 8562–8566.
3. Chen, Z.; Cotterell, B.; Wang, W.; Guenther, E.; Chua, S.-J. A Mechanical Assessment of Flexible Optoelectronic Devices. *Thin Solid Films* **2001**, *394*, 202–206.
4. TFT LCD Makers Drive Indium Shortage and Evade It. *III−Vs Rev.* **2005**, *18*, 12.
5. Geng, H.-Z.; Kim, K. K.; So, K. P.; Lee, Y.-S.; Chang, Y. C.; Lee, Y. H. Effect of Acid Treatment on Carbon Nanotube-Based Flexible Transparent Conducting Films. *J. Am. Chem. Soc.* **2007**, *129*, 7758–7759.
6. Kang, M.-G.; Guo, L. J. Nanoimprinted Semitransparent Metal Electrodes and Their Application in Organic Light-Emitting Diodes. *Adv. Mater.* **2007**, *19*, 1391–1396.
7. Lee, J.-Y.; Connor, S. T.; Cui, Y.; Peumans, P. Solution-Processed Metal Nanowire Mesh Transparent Electrodes. *Nano Lett.* **2008**, *8*, 689–692.
8. Koch, N.; Elschner, A.; Johnson, R. L.; Rabe, J. P. Energy Level Alignment at Interfaces with Pentacene: Metals *versus* Conducting Polymers. *Appl. Surf. Sci.* **2005**, *244*, 593–597.
9. Yang, Y.; Heeger, A. J. Polyaniline as a Transparent Electrode for Polymer Light-Emitting Diodes: Lower Operating Voltage and Higher Efficiency. *Appl. Phys. Lett.* **1994**, *64*, 1245–1247.
10. Kim, J.-Y.; Woo, H.-Y.; Baek, J.-W.; Kim, T.-W.; Song, E.-A.; Park, S.-C.; Ihm, D.-W. Polymer-Dispersed Liquid Crystal Devices Using Highly Conducting Polymers as Electrodes. *Appl. Phys. Lett.* **2008**, *92*, 183301-1–188330-3.
11. Becerril, H. A.; Mao, J.; Liu, Z.; Stoltenberg, R. M.; Bao, Z.; Chen, Y. Evaluation of Solution-Processed Reduced Graphene Oxide Films as Transparent Conductors. *ACS Nano* **2008**, *2*, 463–470.
12. Fuhrer, M. S.; Nygård, J.; Shih, L.; Forero, M.; Yoon, Y.-G.; Mazzoni, M. S. C.; Choi, H. J.; Ihm, J.; Louie, S. G.; Zettl, A.; McEuen, P. L. Crossed Nanotube Junctions. *Science* **2000**, *288*, 494–497.
13. Green, A. A.; Hersam, M. C. Colored Semitransparent Conductive Coatings Consisting of Monodisperse Metallic Single-Walled Carbon Nanotubes. *Nano Lett.* **2008**, *8*, 1417–1422.
14. Blackburn, J. L.; Barnes, T. M.; Beard, M. C.; Kim, Y.-H.; Tenent, R. C.; McDonald, T. J.; To, B.; Coutts, T. J.; Heben, M. J. Transparent Conductive Single-Walled Carbon Nanotube Networks with Precisely Tunable Ratios of Semiconducting and Metallic Nanotubes. *ACS Nano* **2008**, *2*, 1266–1274.
15. Yanagi, K.; Miyata, Y.; Kataura, H. Optical and Conductive Characteristics of Metallic Single-Wall Carbon Nanotubes with Three Basic Colors; Cyan, Magenta, and Yellow. *Appl. Phys. Express* **2008**, *1*, 034003-1–034003-3.
16. Zhang, M.; Fang, S.; Zakhidov, A. A.; Lee, S. B.; Aliev, A. E.; Williams, C. D.; Atkinson, K. R.; Baughman, R. H. Strong, Transparent, Multifunctional, Carbon Nanotube Sheets. *Science* **2005**, *309*, 1215–1219.
17. Hone, J.; Llaguno, M. C.; Nemes, N. M.; Johnson, A. T.; Fischer, J. E.; Walters, D. A.; Casavant, M. J.; Schmidt, J.; Smalley, R. E. Electrical and Thermal Transport Properties of Magnetically Aligned Single Wall Carbon Nanotube Films. *Appl. Phys. Lett.* **2000**, *77*, 666–668.
18. Fischer, J. E.; Zhou, W.; Vavro, J.; Llaguno, M. C.; Guthy, C.; Haggenmueller, R.; Casavant, M. J.; Walters, D. E.; Smalley, R. E. Magnetically Aligned Single Wall Carbon Nanotube Films: Preferred Orientation and Anisotropic Transport Properties. *J. Appl. Phys.* **2003**, *93*, 2157–2163.
19. Parekh, B. B.; Fanchini, G.; Eda, G.; Chhowalla, M. Improved Conductivity of Transparent Single-Wall Carbon Nanotube Thin Films via Stable Postdeposition Functionalization. *Appl. Phys. Lett.* **2007**, *90*, 121913-1–121913-3.
20. Jackson, R.; Domercq, B.; Jain, R.; Kippelen, B.; Graham, S. Stability of Doped Transparent Carbon Nanotube Electrodes. *Adv. Func. Mater.* **2008**, *18*, 2548–2554.
21. Dettlaff-Weglikowska, U.; Skákalová, V.; Graupner, R.; Jhang, S. H.; Kim, B. H.; Lee, H. J.; Ley, L.; Park, Y. W.; Berber, S.; Tománek, D.; Roth, S. Effect of $SOCl_2$ Treatment on Electrical and Mechanical Properties of Single-Wall Carbon Nanotube Networks. *J. Am. Chem. Soc.* **2005**, *127*, 5125–5131.
22. Wu, Z.; Chan, Z.; Du, X.; Logan, J. M.; Sippel, J.; Nikolou, M.; Kamaras, K.; Reynolds, J. R.; Tanner, D. B.; Hebard, A. F.; Rinzler, A. G. Transparent, Conductive Carbon Nanotube Films. *Science* **2004**, *305*, 1273–1276.
23. Zhou, Y.; Hu, L.; Grüner, G. A Method of Printing Carbon Nanotube Thin Films. *Appl. Phys. Lett.* **2006**, *88*, 123109-1–123109-3.
24. Hilt, O.; Brom, H. B.; Ahlskog, M. Localized and Delocalized Charge Transport in Single-Wall Carbon-Nanotube Mats. *Phys. Rev. B.* **2000**, *61*, R5129–R5132.
25. Zhang, D.; Ryu, K.; Liu, X.; Polikarpov, E.; Ly, J.; Tompson, M. E.; Zhou, C. Transparent, Conductive, and Flexible Carbon Nanotube Films and Their Application in Organic Light-Emitting Diodes. *Nano Lett.* **2006**, *6*, 1880–1886.
26. De, S.; Lyons, P. E.; Sorel, S.; Doherty, E. M.; King, P. J.; Blau, W. J.; Nirmalraj, P. N.; Boland, J. J.; Scardaci, V.; Joimel, J; Coleman, J. Transparent, Flexible, and Highly Conductive Thin Films Based on Polymer-Nanotube Composites. *ACS Nano* **2009**, *3*, 714–720.
27. Kaempgen, M.; Duesberg, G. S.; Roth, S. Transparent Carbon Nanotube Coatings. *Appl. Surf. Sci.* **2005**, *252*, 425–429.
28. Dan, B.; Irvin, G. C.; Pasquali, M. Continuous and Scalable Fabrication of Transparent Conducting Carbon Nanotube Films. *ACS Nano* **2009**, *3*, 835–843.
29. Yim, J. H.; Kim, Y. S.; Koh, K. H.; Lee, S. Fabrication of Transparent Single Wall Carbon Nanotube Films with Low Sheet Resistance. *J. Vac. Sci. Technol., B* **2008**, *26*, 851–855.
30. Ikeda, A.; Nobusawa, K.; Hamano, T.; Kikuchi, J. Single-Walled Carbon Nanotubes Template the One-Dimensional Ordering of a Polythiophene Derivative. *Org. Lett.* **2006**, *8*, 5489–5492.
31. Geng, J.; Kong, B.-S.; Yang, S. B.; Youn, S. C.; Park, S.; Joo, T.; Jung, H.-T. Effect of SWNT Defects on the Electron Transfer Properties in P3HT/SWNT Hybrid Materials. *Adv. Funct. Mater.* **2008**, *18*, 2659–2665.
32. Kymakis, E.; Amaratunga, G. A. J. Single-Wall Carbon Nanotube/Conjugated Polymer Photovoltaic Devices. *Appl. Phys. Lett.* **2002**, *80*, 112–114.

33. Geng, J.; Zeng, T. Influence of Single-Walled Carbon Nanotubes Induced Crystallinity Enhancement and Morphology Change on Polymer Photovoltaic Devices. *J. Am. Chem. Soc.* **2006**, *128*, 16827–16833.
34. Wang, W.; Shiral Fernando, K. A.; Lin, Y.; Meziani, M.; Monica Veca, L.; Cao, L.; Zhang, P.; Kimani, M. M.; Sun, Y.-P. Metallic Single-Walled Carbon Nanotubes for Conductive Nanocomposites. *J. Am. Chem. Soc.* **2008**, *130*, 1415–1419.
35. Gu, H.; Swager, T. M. Fabrication of Free-standing, Conductive, and Transparent Carbon Nanotube Films. *Adv. Mater.* **2008**, *20*, 4433–4437.
36. LeMieux, M. C.; Roberts, M.; Barman, S.; Jin, Y. W.; Kim, J. M.; Bao, Z. Self-Sorted, Aligned Nanotube Networks for Thin-Film Transistors. *Science* **2008**, *321*, 101–104.
37. Geng, H.-Z.; Lee, D. S.; Kim, K. K.; Kim, S. J.; Bae, J. J.; Lee, Y. H. Effect of Carbon Nanotube Types in Fabricating Flexible Transparent Conducting Films. *J. Korean Phys. Soc.* **2008**, *53*, 979–985.
38. Kataura, H.; Kumazawa, Y.; Maniwa, Y.; Umezu, I.; Suzuki, S.; Ohtsuka, Y.; Achiba, Y. Optical Properties of Single-Wall Carbon Nanotubes. *Synth. Met.* **1999**, *103*, 2555–2558.
39. Li, Z.; Kandel, H. R.; Dervishi, E.; Saini, V.; Xu, Y.; Biris, A. R.; Lupu, D.; Salamo, G. J.; Biris, A. S. Comparative Study on Different Carbon Nanotube Materials in Terms of Transparent Conductive Coatings. *Langmuir* **2008**, *24*, 2655–2662.
40. Barnes, T. M.; Blackburn, J. L.; van de Lagemaat, J.; Coutts, T. J.; Heben, M. J. Reversibility, Dopant Desorption, and Tunneling in the Temperature-Dependent Conductivity of Type-Separated, Conductive Carbon Nanotube Networks. *ACS Nano* **2008**, *2*, 1968–1976.
41. Jorio, A.; Pimenta, M. A.; Fantini, C.; Souza, M.; Souza Filho, A. G.; Samsonidze, Ge. G.; Dresselhaus, G.; Dresselhaus, M. S.; Saito, R. Advances in Single Nanotube Spectroscopy: Raman Spectra from Cross-Polarized Light and Chirality Dependence of Raman Frequencies. *Carbon* **2004**, *42*, 1067–1069.
42. Lefrant, S.; Baltog, I.; Lamy de la Chapelle, M.; Baibarac, M.; Louarn, G.; Journet, C.; Bernier, P. Structural Properties of Some Conducting Polymers and Carbon Nanotubes Investigated by SERS Spectroscopy. *Synth. Met.* **1999**, *100*, 13–27.
43. Zimney, E. J.; Dommett, G. H. B.; Ruoff, R. S.; Dikin, D. Correction Factors for 4-Probe Electrical Measurements with Finite Size Electrodes and Material Anisotropy: A Finite Element Study. *Meas. Sci. Technol.* **2007**, *18*, 2067–2073.
44. Hu, L.; Hecht, D. S.; Gruner, G. Percolation in Transparent and Conducting Carbon Nanotube Networks. *Nano Lett.* **2004**, *4*, 2513–2517.